Static and dynamic properties of the classical XY chain

R. W. Gerling* and D. P. Landau
Department of Physics and Astronomy, University of Georgia, Athens, Georgia 30602
(Received 12 April 1982)

We present results for the static and dynamic behavior of a one-dimensional classical XY chain. Equilibrium configurations are produced by an importance-sampling Monte Carlo method. Static properties are evaluated from these data and a spin-dynamics method is then used to evaluate time-displaced correlation functions and to calculate the scattering function $S(q,\omega)$. The transverse spin-spin correlation functions decay exponentially for large times. The longitudinal spin-spin correlation functions show oscillatory behavior, especially at low temperatures. The longitudinal-scattering function displays spin-wave peaks, and the transverse-scattering function shows central peaks (relaxational behavior) which change to fluctuation-broadened spin-wave peaks for large values of q/κ. The energy-energy correlation function shows diffusive behavior for high temperatures and nondiffusive behavior for low temperatures.

I. INTRODUCTION

The interest in the properties of one-dimensional magnetic systems has been great over the years[1–7] because their study helps provide understanding of the more complex theory of higher-dimensional systems. The first exact solution of a classical one-dimensional system was given by Ising,[1] and a solution of the classical Heisenberg model[2] showed similar qualitative behavior. Since the discovery of real pseudo-one-dimensional magnetic systems[3] there has been renewed activity in the field of one-dimensional magnetic systems. Lurie *et al.*[5] reported simulation results for the dynamics of the classical Heisenberg model and Huber[6] did the same for the classical XY model at infinite temperature. Landau and Thomchick[7] reported more detailed spin-dynamic results for the classical XY model at both finite and infinite temperature; however, their results were only for relatively short times. Nelson and Fisher[4] obtained an analytic solution for a similar model for which the projection of the classical spin vectors onto the XY plane was fixed but the z component could vary. (Hence the lengths of the vectors were not fixed.)

In this paper we want to study the dynamics of the classical XY model by using computer simulation methods. The Hamiltonian is

$$\mathcal{H}=-J\sum_{(i,j)}(S_i^xS_j^x+S_i^yS_j^y)\,, \tag{1}$$

where the sum (i,j) runs over all nearest-neighbor pairs, and the $\vec{S}_i$ are three-dimensional classical vectors of unit length. (The restriction to nearest-neighbor interaction only is not necessary, and the algorithm can easily be expanded to interactions with more neighbors.) In the classical Heisenberg model the internal energy and the magnetization are constants of the motion. In contrast, in the XY model, the magnetization is not a constant of the motion, and only its z component does not change with time. We, therefore, expect qualitatively different behavior for the XY model.

We used a standard Monte Carlo algorithm and an improved spin-dynamics method to study this model. These methods are described in some detail in Sec. II of this paper. The results are presented in Sec. III, where we also compare our results with earlier work and with analytic results of Nelson and Fisher.[4]

II. METHOD

To obtain equilibrium spin configurations we used an importance-sampling Monte Carlo method.[8] We took spin chains with periodic boundary conditions with $N=1000$ and also, to test finite-size effects, with $N=2000$.

Successive spin configurations are generated by reorienting each single spin by the probability

$$p(\vec{S}_i\rightarrow\vec{S}_i')=\exp(-\beta\Delta E)\,, \tag{2}$$

where ΔE is the change in energy resulting from the reorientation of the spin and $\beta=(1/kT)$. At each temperature at least 1500 Monte Carlo steps per spin were performed. The first 500 steps were not retained, allowing the system to reach equilibrium. The remaining steps were used to compute averages of the internal energy, order parameter, and static spin-spin correlation functions. The specific heat was determined from the fluctuations.[9]

Five different spin states separated by 200 Monte Carlo steps are used as starting configurations for a spin-dynamics study. The separation should ensure that the five spin configurations are statistically independent from each other. The equation of motion is derived[3] from the quantum-mechanical equation

$$\frac{d}{dt}\vec{S}_i = i[\mathcal{H},\vec{S}_i] \ . \tag{3}$$

Evaluating the commutator and performing the classical limit, the classical equation of motion reads

$$\frac{d}{dt}S_i^x = -JS_i^z(S_{i+1}^y + S_{i-1}^y) \ , \tag{4a}$$

$$\frac{d}{dt}S_i^y = JS_i^z(S_{i+1}^x + S_{i-1}^x) \ , \tag{4b}$$

$$\frac{d}{dt}S_i^z = J[S_i^x(S_{i+1}^y + S_{i-1}^y) - S_i^y(S_{i+1}^x + S_{i-1}^x)] \ . \tag{4c}$$

Here we explicitly take into account only the nearest-neighbor interaction. Otherwise one has to replace the $+1$ and the -1 by a sum over all neighbor interactions which are included.

The integration of Eq. (4) was performed by using the formula[10]

$$\vec{S}_i(t+\Delta) = \vec{S}_i(t-\Delta) + 2\dot{\vec{S}}_i(t)\Delta + \tfrac{1}{3}\dddot{\vec{S}}_i(t)\Delta^3 + O(\Delta^5) + \cdots \ , \tag{5}$$

where Δ is the time interval of the integration. This formula can be derived easily from a simple Taylor expansion up to fourth order. The error is of the order Δ.[5] To obtain $\dddot{\vec{S}}$ we must differentiate Eq. (4) twice with respect to time. From each of the five time integrations per temperature time-displaced correlation functions are extracted:

$$\langle E_i(0)E_i(t)\rangle = \frac{-J^2}{N}\sum_i [S_i^x(0)S_{i+1}^x(0) + S_i^y(0)S_{i+1}^y(0)][S_i^x(t)S_{i+1}^x(t) + S_i^y(t)S_{i+1}^y(t)] \ , \tag{6a}$$

$$\langle S_i(0)S_{i+r}(t)\rangle_\perp = \frac{1}{N}\sum_i [S_i^x(0)S_{i+r}^x(t) + S_i^y(0)S_{i+r}^y(t)] \ , \tag{6b}$$

$$\langle S_i(0)S_{i+r}(t)\rangle_{||} = \frac{1}{N}\sum_i S_i^z(0)S_{i+r}^z(t) \ , \tag{6c}$$

Using a time increment $\Delta = 0.005J^{-1}$ we integrated out to time $t = 30J^{-1}$. Longer times could be investigated by using smaller time increments (to increase the accuracy) and more time steps. Carrying out the time integration and calculating the correlation functions takes about 38 min on a Control Data Corp. CYBER 170/730 for a 1000-spin chain.

The energy and the z component of the order parameter are constants of motion, so we can take these quantities as rough indicators of the quality of the dynamical data. To check these we have printed both quantities up to five significant digits. We cannot see any variation with time up to time $t = 30J^{-1}$. To find out about the influence of the length of the time increment Δ we integrated single configurations with different increments. Using, for example, $\Delta = 0.02J^{-1}$ out to time $t = 120J^{-1}$ we see the first variation in the fifth digit of the energy at time $t = 100J^{-1}$. From that viewpoint the data look very good. But there is another check for quality of the data: The time-displaced energy-energy correlation function (6a). Regarding this quantity we can say that with $\Delta = 0.02J^{-1}$ the time integration starts to become poor around $t = 12J^{-1}$. At times $t = 30J^{-1}$, $\Delta = 0.005J^{-1}$ is the best compromise between the accuracy of the integration and the running time of the program. In addition, in a few cases we checked the length change of the spin vectors during the time integration. For $\Delta = 0.005J^{-1}$ the average length change was found to be smaller than 0.02% during a run. Our tests indicate that the integration routine works extremely well and that one can neglect the errors from the numerical time integration compared with the errors resulting from the use of a small number of starting configurations.

The last step in the computer program performs a double Fourier transform of the spin-spin correlation functions. To reduce cutoff effects we introduced a Gaussian spatial and temporal resolution function.[11,12] We first performed the space Fourier transform by

$$\langle S(-q,0)S(q,t)\rangle_k = \sum_r \cos qr \langle S_i(0)S_{i+r}(t)\rangle_k \times \exp\left[-\frac{1}{2}\left[\frac{r}{\Delta r}\right]^2\right] \quad (k = \perp, ||) \ . \tag{7}$$

The sum over r runs typically over 100 neighbors. The cutoff parameter Δr was chosen to be 0.03. After this we determined the time Fourier transform by

$$S_k(q,\omega)=\int_0^\infty \cos\omega t \,\langle S(-q,0),S(q,t)\rangle_k \times\exp\left[-\frac{1}{2}\left[\frac{t}{\Delta t}\right]^2\right]dt \qquad (8)$$

$(k=\perp,\|)$.

This integration was performed numerically and the time cutoff parameter Δt was chosen differently to find the best value. If Δt is too small we get large oscillations in the scattering function, if it is too large all structure is smeared out. We obtained best results with $\Delta t=0.1J^{-1}$.

III. RESULTS

A. Static properties

The static data for the classical XY chain show a nonsingular behavior at all temperatures. Figure 1 shows the temperature dependence of the internal energy and of the specific heat. For small temperatures ($T\leq 0.1J/k$) the internal energy is proportional to T. This agrees with the asymptotic $T\to 0$ form given by Joyce.[13] In contrast to the behavior for the Heisenberg chain the internal energy increases above the $T\to 0$ asymptote as T increases. This leads to a broad Schottky-type maximum in the specific heat.

Figure 2 shows the results of the transverse susceptibility. Joyce[13] predicted that χT should be proportional to T^{-1} for $T\to 0$. To see this we have plotted χT against the temperature. For temperature $T<0.1J/k$ we found this asymptotic behavior. In the temperature range between $0.1J/k$ and $0.2J/k$ (where the specific heat shows a maximum) χT starts to deviate from the asymptotic behavior and decreases by 1 order of magnitude. For temperatures between $0.3J/k$ and $5.0J/k$, χT approaches the Curie law. For $T>5.0J/k$ the transverse susceptibility obeys the Curie law.

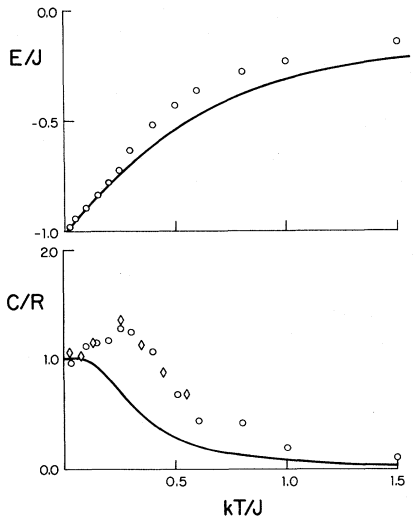

FIG. 1. Temperature dependence of the internal energy E/J and the specific heat C/R. The circles are data from the Monte Carlo calculation. The diamonds in the specific-heat data are obtained from a numerical differentiation of the internal energy data. The solid lines are exact results for the classical Heisenberg chain (Ref. 2).

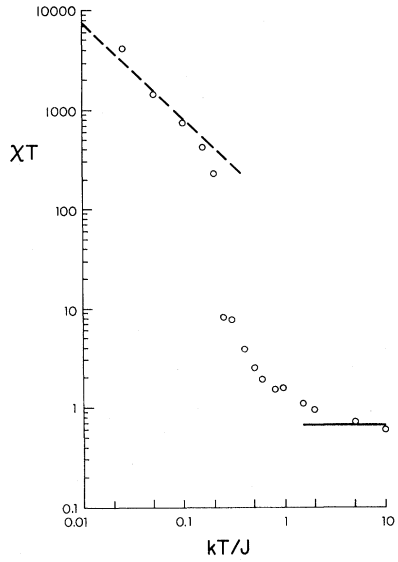

FIG. 2. Temperature dependence of the transverse susceptibility χT. The circles are from the Monte Carlo calculation. The dashed line is the asymptotic form given by Joyce (Ref. 13). The solid line is the Curie law.

The spin-spin correlation function should decay exponentially with distance.[4,14] Figure 3 shows in the upper part of the spin-spin correlation function for $T=0.2J$. Wegner[14] also calculated that the inverse correlation length κ is given by

$$\kappa=\frac{kT}{2J} . \qquad (9)$$

To obtain results for the inverse correlation length we fitted an exponential to the spin-spin correlation function as shown in Fig. 3(a). The results for κ are given in Fig. 3(b). For temperatures $T<0.2J/k$ we found the temperature dependence given by Eq. (9). Again the deviations start around the temperature where the maximum of the specific heat occurs.

B. Dynamic behavior

Figure 4 shows the reduced time-dependent energy-energy correlation function. For high temperatures the correlations decay as $t^{-1/2}$ for $Jt>1.0$ indicating diffusive behavior. The diffusion constant shows a slow temperature dependence. This is in agreement with the findings of Landau and

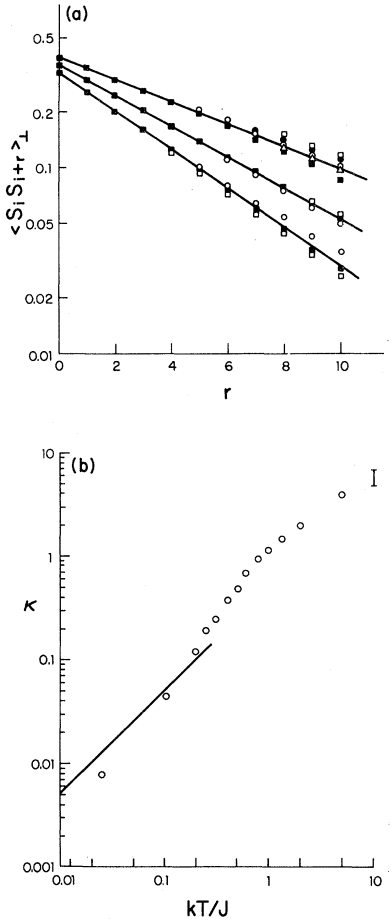

FIG. 3. (a) r dependence of the spin-spin correlation function for temperature $T=0.2J$, $T=0.25J$, and $T=0.3J$ (from top to bottom). Different symbols show data from different simulations. The solid lines show best fits. (b) Temperature dependence of the inverse correlation length. The circles are the data from the simulations. The solid line is the result given by Wegner (Ref. 14). The error is of the order of the symbol size, except for the point for the lowest temperature. That error is larger, but we cannot give an estimate for it.

Thomchick.[7]

The situation is quite different for low temperatures. As an example, in Fig. 4 we show the results for $T=0.2J/k$. The best fit to this curve is a $t^{-\alpha}$ behavior with α between 0.8 and 0.9. There are noticeable differences in the data for different runs. In addition, the diffusion constant shows a stronger temperature dependence. (Lurie *et al.*[6] did not find a $t^{-1/2}$ behavior in their results for a classical Heisenberg chain either.)

Nelson and Fisher[4] gave an expression for the transverse spin-spin correlation function in their pseudo-XY chain:

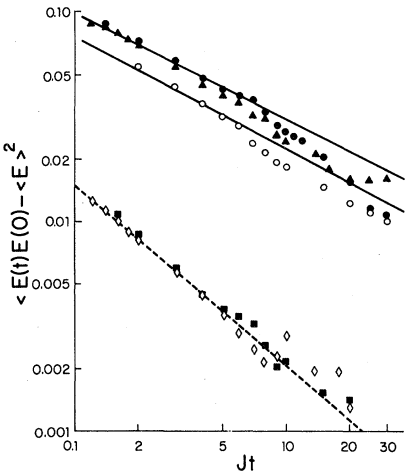

FIG. 4. Time dependence of the energy-energy correlation function. The symbols denote: (▲) $T=\infty$, $N=1000$, 5 runs, $\Delta=0.005J^{-1}$; (●) $T=\infty$, $N=2000$, 1 run, $\Delta=0.02J^{-1}$; (○) $kT=0.5J$, $N=1000$, 5 runs, $\Delta=0.01J^{-1}$; (■) $kT=0.2J$, $N=1000$, 5 runs, $\Delta=0.01J^{-1}$; (◇) $kT=0.2J$, $N=2000$, 1 run, $\Delta=0.05J^{-1}$. The solid lines have slope $-\frac{1}{2}$, the dashed line is a best fit.

$$S_\perp(r,t)=\exp\left[-\frac{\kappa}{2}(\,|r-ct|+|r+ct|\,)\right], \tag{10}$$

where κ is the inverse correlation length and c is the spin-wave velocity.

The correlation function $S_\perp(r,t)$ reflects for $t=0$ the spatial exponential decay we discussed in Sec. III A. For times $t<r/c$ the correlation function remains constant and then for times $t>r/c$ it decays exponentially. Figure 5(a) shows a comparison between the analytic function $S_\perp(r,t)$ and our results from the spin-dynamics calculation. We only show data for $Jt\leq 14$ so that the short-time small-r results can be clearly resolved. The parameter κ is taken

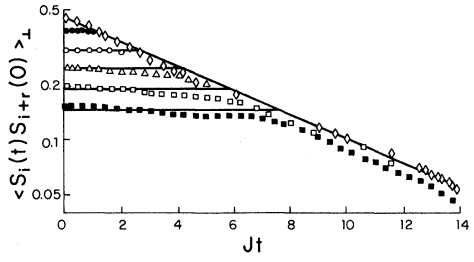

FIG. 5. Transverse spin-spin correlation function $\langle S_i(t)S_{i+r}(0)\rangle_\perp$. The symbols denote: (◇) $r=0$, (●) $r=1$, (○) $r=3$, (△) $r=5$, (□) $r=7$, and (■) $r=9$. The solid lines are calculated from Eq. (10). The temperature is $kT=0.2J$.

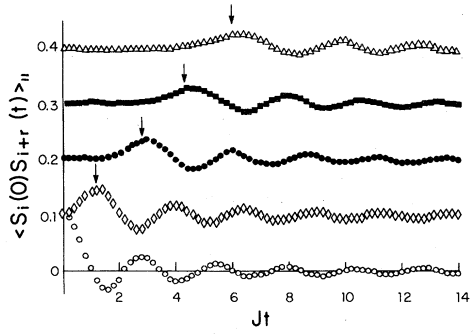

FIG. 6. Longitudinal spin-spin correlation function $\langle S_i(t)S_{i+r}(0)\rangle_{||}$. The symbols denote (○) $r=0$, (◇) $r=1$, (●) $r=3$, (■) $r=5$, and (△) $r=7$. For clarity the zero line is shifted 0.1 for the different cases. The temperature is $kT=0.2J$. The small arrows show predicted propagation times $t=r/c$.

from the static data, and the spin-wave velocity c is taken from the initial slope of the dispersion relation which we will show in Fig. 8. The spin-dynamics picture of Nelson and Fisher[4] is in good agreement with our data. The constant behavior of $S_{\perp}(r,t)$ is understandable since a spin wave needs time to travel from spin i to spin $i+r$. During this time the correlation cannot decay.

Figure 6 shows the longitudinal spin-spin correlation function $s_{||}(r,t)$. Especially at low temperatures we see pronounced oscillations. These oscillations can still be seen in the data for $Jt<14$ but cannot be resolved in the figure using legible symbols. Even for $T=\infty$ we can see remnants of these oscillations in our results. We can see essentially the same spin-wave velocity in these. The small arrows indicate the times $t=r/c$ for the different values of r. This shows that in both polarizations the spin waves propagate with the same velocity. The t components of spins are uncorrelated for times $t<r/c$. After this time, when the spin wave has traveled the distance r they become correlated. The correlation function shows the damped oscillations of the longitudinal spin component.

The expression (10) for the transverse spin-spin correlation function can be Fourier transformed. The result is[4]

$$S_{\perp}(q,\omega)=\frac{1}{c}\frac{8\kappa^2}{\left[\kappa^2+\left[\frac{\omega}{c}-q\right]^2\right]\left[\kappa^2+\left[\frac{\omega}{c}+q\right]^2\right]}, \tag{11}$$

where κ and c are the inverse correlation length and the spin-wave velocity, respectively.

The scattering function $S_{\perp}(q,\omega)$ has poles at the complex frequencies

$$\omega_{\pm}(q)=\pm cq+ic\ . \tag{12}$$

According to Nelson and Fisher[4] the frequencies ω should obey dynamic scaling

$$\omega_{\pm}(q)=q^z\Omega_{\pm}(q/\kappa) \tag{13}$$

with

$$z=1,\quad \Omega_{\pm}(x)=c\left[\pm 1+\frac{i}{x}\right]. \tag{14}$$

To test these relations we have plotted the scattering function $S_{\perp}(q,\omega)$ in Fig. 7.

We see more or less the qualitative behavior of Eq. (11). The central peak for $q=0$ is strongly pronounced. For higher q values it is difficult to see the spin-wave peaks. They are broadened by the fluctuations and in the same way their intensity is decreased. Nevertheless, we were able to determine the position of the spin-wave peaks. The two peaks seen for $q=0$ and $\omega>0$ are artificial effects due to

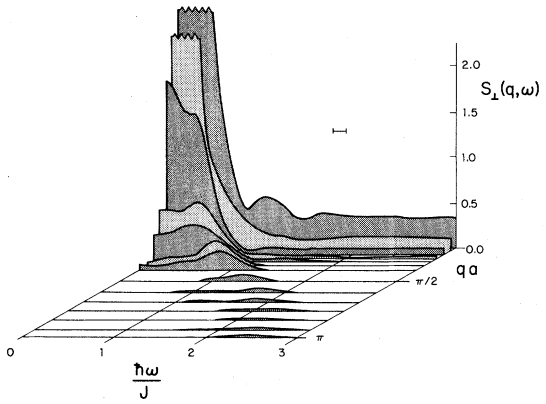

FIG. 7. Transverse scattering function $S_{\perp}(q,\omega)$. The bar indicates the width of the resolution function.

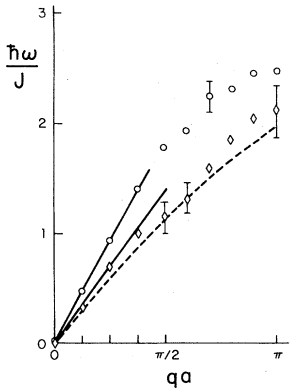

FIG. 8. Dispersion relation $\omega(q)$ for $kT=0.2J$ (○) and $kT=0.5J$ (◇). The straight lines are "best fits" through the points with $qa<\pi/2$. The dashed line shows an estimate for $T=\infty$.

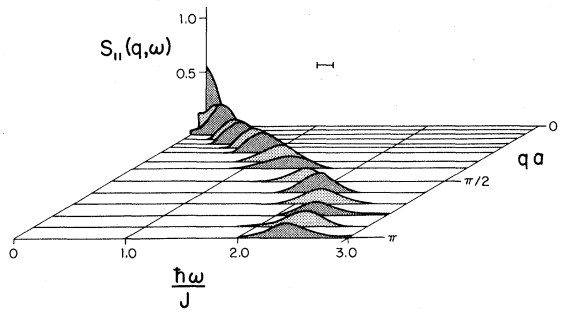

FIG. 9. Longitudinal scattering function $S_{||}(q,\omega)$ for the same q values as in Fig. 7. The bar indicates the width of the resolution function.

limitations in the computer simulation. They are very small compared with the height of peak at $q=0$ and $\omega=0$ [$S_{\perp}(q=0,\omega=0)=25.7$]. The effects do not result from a poor spin-dynamics routine but rather from the finite number of starting configurations (for chains of finite length) we have chosen for the spin-dynamics simulation. When we average only over three different runs, we see some results with much more pronounced spurious peaks, and others without any. To eliminate these effects we should simulate longer chains, and average over more different runs. (However, such a procedure requires much more computer time and hence would be much more expensive.)

Figure 8 shows a test of the dynamic scaling relation. We have taken the positions of the spin-wave peaks from the scattering function. For $qa \leq \pi/2$ the dynamics scaling relation is fulfilled quite well, but for $qa \geq \pi/2$ there are large deviations from that linear relation. (The spin-wave velocity in the analytic expression of Fig. 5 is taken from the linear region of this dynamic scaling relation.)

Figure 9 shows the longitudinal component of the scattering function $S_{||}(q,\omega)$. For $q=0$ we see a narrow line at $\omega=0$ (the width is totally due to the width of resolution function). For $q\neq 0$ we see slightly broadened spin-wave peaks with a width independent of q. The position of these spin-wave peaks is within the statistical error the same as in the transverse scattering law. This reflects the same spin-wave velocity in both polarizations.

IV. CONCLUSION

For the classical XY chain we find static behavior which shows pronounced short-range-order effects. This is expressed mainly in a broad Schottky-type maximum in the specific heat around $T=0.25J$ and a large change in the susceptibility at the same temperature. The dynamic data reflect very nice spin-wave behavior for both polarizations. The results for the transverse components are in very good agreement with predictions by Nelson and Fisher.[4] Only the dynamic scaling relation for $qa > \pi/2$ does not hold. We also found that the spin-wave dispersion relation is the same for both polarizations, including the deviation from the linear dynamic scaling relation for $qa > \pi/2$.

Our results also indicate that substantial improvement in the accuracy and resolution of the scattering function can be obtained only if the time integration is extended to much longer times. This requires an improved algorithm, or smaller time interval, which produces extremely accurate values for the time-displaced correlation functions.

ACKNOWLEDGMENTS

This research was supported in part by NSF Grant No. DMR 7926178. One of us (R.W.G.) also wishes to thank the Fulbright Commission for the award of a travel grant.

*Permanent address: Institut für Theoretische Physik, Universität Erlangen-Nürnberg, Glückstrasse 6, 8520 Erlangen, West Germany.

[1]E. Ising, Z. Phys. 31, 253 (1925).
[2]M. E. Fisher, Am. J. Phys. 32, 343 (1964).
[3]M. Steiner, J. Villain, and C. G. Windsor, Adv. Phys. 25, 87 (1976).
[4]D. R. Nelson and D. S. Fisher, Phys. Rev. B 16, 4945 (1977).
[5]N. A. Lurie, D. L. Huber, and M. Blume, Phys. Rev. B 9, 2171 (1974).
[6]D. L. Huber, Phys. Rev. B 10, 2955 (1974).
[7]D. P. Landau and J. Thomchick, J. Appl. Phys. 50, 1822 (1979).
[8]K. Binder and D. P. Landau, Phys. Rev. B 13, 1140 (1976).
[9]See, e.g., L. D. Landau and E. M. Lifshitz, *Statistical Physics*, Vol. 5 of *Course of Theoretical Physics* (Pergamon, Oxford, 1969).
[10]R. H. Morf and E. P Stoll, in *Numerical Analysis*, edited by J. Descloux and J. Marti (Birkhauser, Basel, 1977).
[11]T. R. Koehler and P. A. Lee, J. Comp. Phys. 22, 319 (1976).
[12]The introduction of this resolution function (or "window function") is equivalent to introducing a finite-resolution function in neutron scattering where data obtained are averages over a finite range of energy and momentum.
[13]G. S. Joyce, Phys. Rev. Lett. 19, 581 (1967).
[14]F. Wegner, Z. Phys. 206, 465 (1967).